American Journal of Botany 96(2): 409–419. 2009.

Morphological variation of intervessel pit membranes and implications to xylem function in angiosperms[1]

Steven Jansen,[2,4] Brendan Choat,[3] and Annelies Pletsers[2]

[2]Jodrell Laboratory, Royal Botanic Gardens, Kew, Richmond, TW9 3DS, Surrey, UK; and [3]Functional Ecology Group, Research School of Biological Sciences, Australian National University, Canberra, ACT 2601, Australia

Pit membranes between xylem vessels have been suggested to have functional adaptive traits because of their influence on hydraulic resistance and vulnerability to embolism in plants. Observations of intervessel pit membranes in 26 hardwood species using electron microscopy showed significant variation in their structure, with a more than 25-fold difference in thickness (70–1892 nm) and observed maximum pore diameter (10–225 nm). In some SEM images, pit membrane porosity was affected by sample preparation, although pores were resolvable in intact pit membranes of many species. A significant relationship ($r^2 = 0.7$, $P = 0.002$) was found between pit membrane thickness and maximum pore diameter, indicating that the thinner membranes are usually more porous. In a subset of nine species, maximum pore diameter determined from SEM was correlated with pore diameter calculated from air-seeding thresholds ($r^2 = 0.8$, $P < 0.001$). Our data suggest that SEM images of intact pit membranes underestimate the porosity of pit membranes in situ. Pit membrane porosity based on SEM offers a relative estimate of air-seeding thresholds, but absolute pore diameters must be treated with caution. The implications of variation in pit membrane thickness and porosity to plant function are discussed.

Key words: bordered pit; cavitation; embolism; hardwoods; pit membrane; vessel element; wood anatomy; xylem.

In the xylem tissue of hardwood species, water and nutrients are transferred between vessels through bordered pits. As water moves from the roots to the leaves it must traverse intervessel pit membranes hundreds or thousands of times. It has long been recognized that pit membranes play a pivotal role in maintaining the integrity of the water transport system in plants (Zimmermann and Brown, 1971). While allowing the passage of water between xylem vessels, pit membranes must also protect the plant against the spread of gas (embolism) or pathogens through the vascular system (Tyree and Sperry, 1989; Choat et al., 2008). Thus, pit membrane structure must balance the competing functional requirements of minimizing vascular resistance, which favors thin, porous membranes, and limiting the spread of embolism and microbes, which requires robust membranes and smaller pores.

Much attention has been paid to pit membrane ultrastructure of conifer species, in which the conductive and protective functions of the membranes have been spatially resolved into the margo and torus regions (e.g., Liese and Fahnenbrock, 1952; Petty and Preston, 1969; Thomas, 1969; Bauch et al., 1972; Dute et al., 2008). The occurrence and structure of torus-margo pit membranes in angiosperms has also been the focus of several studies, although this pit membrane type is rare in angiosperms (Ohtani and Ishida, 1978; Dute and Rushing, 1987; Dute et al., 2004; Jansen et al., 2004a, 2007). Less anatomical work has focused on the "homogeneous" membranes characteristic of hardwood species, which have a relatively uniform density of microfibrils across the membrane (Schmid, 1965). Early studies emphasized differences between the ultrastructure of intervessel pit membranes and other types of pit membranes (e.g., vessel parenchyma), but indicated little variation in intervessel pit membranes of species examined (Schmid, 1965; Schmid and Machado, 1968; Yang, 1978, 1986). Because preparation of samples for transmission electron microscopy (TEM) is time consuming, most studies include only a few species. Published TEM observations of angiosperm pit membranes are indeed restricted to fewer than a dozen species of hardwoods (Wheeler, 1983). More recently, scanning electron microscope (SEM) studies by Sano (2004, 2005) revealed considerable differences in the structure of intervessel pit membranes of four hardwood species. Such variation in pit membrane structure is predicted to have important consequences for vascular function.

Physiological studies have demonstrated that pit membranes are responsible for at least 50% of the hydraulic resistance in the xylem (Wheeler et al., 2005; Choat et al., 2006; Hacke et al., 2006). Changes in the thickness and porosity of the pit membranes therefore have the potential to exert significant influence over the total hydraulic resistance in the plant. The porosity of pit membranes is also related to the vulnerability of xylem to water stress induced embolism; it is generally believed that water-stress induced cavitation occurs as a result of gas being drawn through pit membrane pores, a process known as air seeding (Zimmermann, 1983; Tyree and Sperry, 1989). Larger pit membrane pores should allow embolism to spread through the xylem at lower tensions (higher xylem water potentials) than smaller pores. Species with more porous membranes, or with more pit membrane area between vessels, will therefore be more prone to vascular dysfunction in the face of water stress. The increase in hydraulic resistance resulting from xylem embolism can impact leaf water status and gas exchange, ultimately resulting in die back of affected organs or the whole plant (Rood et al., 2000). Therefore, the influence of pit membrane structure on both hydraulic resistance and vulnerability to embolism indicate that it is an important adaptive trait with the potential to drive ecological differences between species.

[1] Manuscript received 21 July 2008; revision accepted 25 November 2008.

The authors thank D. Chatelet and T. Rockwell for collecting plant material. This study was supported by a grant from the Royal Society (2006/Rl) and NERC (NE/E001122/1), and a Lennox Boyd fellowship (RBG, Kew). S.J. and B.C. contributed equally to the publication.

[4] Author for correspondence (e-mail: s.jansen@kew.org.uk)

doi:10.3732/ajb.0800248

Despite this, few detailed examinations of pit membrane structure across a wide range of species have been undertaken.

One major concern in studies examining wood micromorphology using electron microscopy is the alteration of ultrastructural features during sample preparation (Choat et al., 2003; Pesacreta et al., 2005; Jansen et al., 2008). For SEM observations, preparation can involve harsh chemical treatments, dehydration of tissue (either air drying or critical point drying) and placement under vacuum during observation. It is reasonable to suspect that subtle features such as pit membrane porosity may have been altered by these processes. Sectioning or splitting of wood sampling may also cause damage to pit membranes. Shane et al. (2000) examined pit membranes of maize roots using cryoSEM to preserve membranes in a hydrated state and reported that pit membranes frequently developed large pores or tears as a result of even partial dehydration before observation. However, some conventional SEM studies have failed to reveal visible pores in the pit membranes of hardwood species (Wheeler, 1981, 1983; Choat et al., 2003). One possible explanation for not observing the pores in pit membranes with SEM is provided by a recent study employing atomic force microscopy (AFM), in which pit membranes were examined in nondried and dried states (Pesacreta et al., 2005). They observed that dried pit membranes had a much more compact appearance compared with that of nondried membranes in which the hydrated microfibrils were loosely arranged. The AFM observations indicate that pores present in hydrated membranes may become obscured by the contraction of microfibrils or redistribution of noncellulosic substances as the membrane dries. Thus, there is some uncertainty over the in situ porosity of pit membranes based on different methods of microscopy.

We undertook an examination of pit membrane structure in 26 hardwood species. We used SEM and TEM because the complementary information offered by these techniques allows for a greater chance of detecting artifacts that may result from preparation, particularly in SEM (Shane et al., 2000; Thorsch 2000). While preparation for the more commonly used SEM technique may cause damage to pit membranes by drying (Jansen et al., 2008), TEM provides an alternative method in which the pit membrane structure is stabilized and supported by resin during sectioning and observation. Observations with SEM and TEM were compared with air-seeding experiments, which provide an estimate of pit membrane pore size in intact and hydrated stem tissue. The species examined included plants from a range of environments including temperate deciduous hardwoods, riparian trees, and Mediterranean evergreens. The principal aims were to determine the level of variation in intervessel pit structure present in these species and to assess the reliability of electron microscopy in assessing pit membrane porosity.

MATERIALS AND METHODS

Plant material—The species studied are listed in Table 1 with reference to their family classification, origin, and collection period. All samples included fresh material from two- to four-year-old branches. All SEM and TEM observations and measurements were based on vessel elements from the current and last year's growth ring to avoid possible degradation or changes in pit porosity and pit membrane structure caused by age or heartwood formation (Wheeler, 1981, 1983; Sano et al., 1999). Between one and three branch samples were studied per species. The few differentiating vessel elements that could be seen in the TEM material collected during spring and summer were easy to distinguish from the fully developed vessel elements with mature pit membranes by the presence of cytoplasm and more electron-dense pit membranes.

Scanning electron microscopy—Wood samples were cut into 5–10 mm lengths, split in half, and dehydrated in an ethanol series of 50%, 70%, 95%, and 100% for 5–30 min in each solution. Samples were air dried for 12 h at room temperature and then split in the tangential or radial plane. The split samples were fixed to aluminum stubs and coated with platinum using an EMITECH K550 sputter coater (Emitech Ltd., Ashford, UK) for 3 min. An electron-conductive carbon paste (Neubauer chemikaliën, Münster, Germany) was used to increase conductivity between the sample and the stage. Samples were observed with a Hitachi S-4700 field-emission scanning electron microscope (Hitachi High Technologies Corp., Tokyo, Japan) at an accelerating voltage of 2 kV. The number of intervessel pit fields examined varied from 5 to >20 per species, depending on the frequency of vessels groupings. Pit membrane porosity, microfibril thickness, and pit membrane diameter were measured on images using ImageJ software (freeware available from website http://rsb.info.nih.gov/ij). In membranes with resolvable pores, average and maximum pore diameters were measured on binary images using the analyze particles function. Pore area was transformed into equivalent circular diameter for each pore detected. Pit characteristics of at least 40 pit membranes were measured.

Transmission electron microscopy—Samples were cut into 2-mm^3 blocks and fixed overnight in Karnovsky's fixative at room temperature (Karnovsky, 1965). After washing in 0.05 M phosphate buffer, the specimens were postfixed in 1% buffered osmium tetroxide for 4 h at room temperature, washed again, and dehydrated through a graded ethanol series (30%, 50%, 70%, 90%, 100%). The ethanol was gradually replaced with LR White resin (London Resin Co., Reading, UK) over several days, with the resin changed approximately every 12 h. The resin was polymerized in a Weiss Gallenkamp (Loughborough, U.K.) vacuum oven at 60°C and 1000 mm Hg for 18–24 h. Embedded samples were trimmed with a razor blade or with a Leica EM specimen trimmer (Leica Microsystems, Vienna, Austria) and sectioned on an ultramicrotome (Ultracut, Reichert-Jung, Vienna, Austria). Transverse sections 1 and 2 μm thick were cut with a glass knife, heat-fixed to glass slides, stained with 0.5% toluidine blue O in 0.1 M phosphate buffer (O'Brien et al., 1964), and mounted in DPX (Agar Scientific, Stansted, UK). Resin-embedded material was prepared for TEM by cutting transverse, ultrathin sections between 60 and 90 nm using a diamond knife. The sections were attached to Formvar grids or 300 mesh hexagonal copper grids (Agar Scientific) and stained with uranyl acetate and lead citrate using an LKB 2168 ultrostainer (LKB-Produkter AB, Bromma, Sweden) or a Leica EM Stain Ultrostainer (Leica Microsystems, Vienna, Austria). Observations were carried out using a JEOL JEM-1210 TEM (JEOL, Tokyo, Japan) at 80 kV accelerating voltage and digital images were taken using a MegaView III camera (Soft Imaging System, Münster, Germany). A minimum of five intervessel pit fields was examined per species. Image analysis was undertaken using ImageJ software with at least 25 measurements for each quantitative pit feature. Variation in membrane thickness was analyzed with a one-way ANOVA, and differences between means were assessed with a Tukey honestly significant difference (HSD) test.

Air-seeding experiments—Branches were collected during August and September 2007 from mature trees growing at the living collections of the Royal Botanic Gardens, Kew. Air-seeding experiments were applied to *Acacia pataczekii*, *Acer negundo*, *Aesculus hippocastanum*, *Betula pendula*, *Laurus nobilis*, *Populus fremontii*, and *Salix alba* and were supplemented with air-seeding values for *Fraxinus americana* and *Sophora japonica* as obtained by Choat et al. (2004) using the same method. We were unable to apply this method to all species studied for microscopy (Table 1) because the vessels were either too narrow (<40 μm) or too long (>30 cm). All branch material was similar in size and age and from the same tree as the samples used for SEM and TEM. The air-seeding threshold for intervessel pit membranes was measured in individual vessels of the last two growth rings as outlined by Melcher et al. (2003) and Choat et al. (2004). Briefly, small branch segments were cut under water from lateral branches, trimmed with a razor blade at each end, and flushed with a filtered (0.22 μm) and degassed 10 mM KCl solution. Most branch segments selected were <1 cm in diameter. For each species, the maximum vessel length was estimated using the air perfusion technique. Because the air-seeding threshold probably depends on the number of end-walls penetrated, we selected segments that were shorter than the maximum vessel length to reduce the possibility that there was more than one end wall. The mean stem length varied from <8 cm in *Betula pendula* to >15 cm in *Acacia pataczekii*, *Cladrastis sinensis*, *Laurus nobilis*, and *Populus fremontii*. Glass microcapillaries (1 μm diameter) were pulled on a pipette puller (Pul1, World Precision Instruments, Sarasota, Florida, USA). The tip

TABLE 1. List of species studied with reference to their family classification, origin, and collection timing.

Species	Family	Origin (accession number)	Time of collection
Acacia pataczekii D.I.Morris	Fabaceae	RBG, Kew (1978–6515)	May 2007 (TEM), June 2007 (SEM)
Acer negundo L.	Sapindaceae	RBG, Kew (1972–930)	November 2005
Acer pseudoplatanus L.	Sapindaceae	RBG, Kew (1963–27203)	November 2006 (TEM), June 2007 (SEM)
Adenocarpus decorticans Boiss.	Fabaceae	RBG, Kew (1995–2238)	May 2007 (TEM), September 2007 (SEM)
Aesculus hippocastanum L.	Sapindaceae	RBG, Kew (1973–18953)	May 2006
Ailanthus altissima Swingle	Simaroubaceae	RBG, Kew (2000–2068)	May 2007 (TEM), June 2007 (SEM)
Arbutus uva-ursii L.	Ericaceae	RBG, Kew (1985–2627)	December 2006 (TEM), March 2007 (SEM)
Betula ermanii Cham.	Betulaceae	RBG, Kew (1996–10)	May 2006
Betula nigra L.	Betulaceae	RBG, Kew (1995–82)	November 2005
Betula pendula Roth.	Betulaceae	RBG, Kew (1995–83)	November 2006 (TEM), March 2007 (SEM)
Citrus reticulata Blanco	Rutaceae	RBG, Kew (1997–5954)	May 2007 (TEM), June 2007 (SEM)
Cordia macrostachya Roem. & Schult.	Boraginaceae	RBG, Kew (1936–31901)	May 2007 (TEM), June 2007 (SEM)
Corylus avellana L.	Betulaceae	RBG, Kew (1969–12913)	November 2006 (TEM), March 2007 (SEM)
Fraxinus americana L.	Oleaceae	RBG, Kew (1967–26809)	November 2005
Ilex aquifolium L.	Aquifoliaceae	RBG, Kew (1973–21154)	May 2007 (TEM), March 2007 (SEM)
Laurus nobilis L.	Lauraceae	RBG, Kew (1973–19372)	November 2005
Olea europaea L.	Oleaceae	RBG, Kew (2005–1588)	May 2007 (TEM), June 2007 (SEM)
Paulownia tomentosa Steud.	Scrophulariaceae	RBG, Kew (2000–4940)	December 2006 (TEM), June 2007 (SEM)
Populus fremontii S.Watts.	Salicaceae	RBG, Kew (1923–62411)	November 2005
Quercus robur L.	Fagaceae	RBG, Kew (1969–16034)	December 2006 (TEM), June 2007 (SEM)
Salix alba L.	Salicaceae	RBG, Kew (1988–2941)	November 2005
Sambucus nigra L.	Caprifoliaceae	RBG, Kew (1985–4643)	November 2006 (TEM), June 2007 (SEM)
Sophora japonica L.	Fabaceae	RBG, Kew (1973–11945)	November 2005
Ulmus americana L.	Ulmaceae	Cambridge University, USA	November 2005
Ulmus procera Salisb.	Ulmaceae	RBG, Kew (without accession no.)	May 2007 (TEM), June 2007 (SEM)
Vitis vinifera L. cv. Chardonnay	Vitaceae	UC Davis	November 2005

of a capillary was broken off, such that the opening of the tip was slightly narrower than the vessel diameter (40–150 μm), and inserted into the lumen of an individual vessel from the last two growth rings using a Leica Wild M8 stereozoom microscope. The tip was then glued in place using cyanoacrylic glue (Loctite 409 gel in combination with Loctite 7455 activator; Henkel Loctite Adhesives Ltd., Welwyn Gardens City, UK). Air was pushed through the vessel at low pressure (ca. 0.1 MPa). We assumed that the vessel was ending in the branch segment and that an intact pit field existed in the sample if no bubbles appeared at the distal end. Samples in which air bubbles streamed out at this pressure were discarded. The pressure threshold required to force gas across intervessel pits field was determined by attaching the glass microcapillary to a pressure source (Model 1000, PMS Instrument, Albany, New York, USA). Nitrogen gas was then applied, and the pressure was increased in 0.1 MPa steps at 1-min intervals until air bubbles appeared at the distal end of the branch as could be seen with a 10× hand lens. A constant flow of small air bubbles was interpreted as the threshold pressure for gas penetration of the intervessel pit membranes between the two vessels.

Theoretical pore diameters (D_T) were calculated from air-seeding thresholds as $D_T = 4\gamma\cos\theta/P_a$, where γ is the surface tension of water and θ is the contact angle at the air–water–membrane interface. The contact angle was treated as 0 because of the hydrophilic nature of pectins coating the cellulose microfibrils. Relationships between variables were plotted as linear regressions or as power laws by log-transforming data when relationships appeared nonlinear (Sokal and Rohlf, 1995).

RESULTS

A survey of quantitative pit characteristics is given in Table 2.

Arrangement and size of intervessel pits—Intervessel pitting was alternate in most samples, with opposite to scalariform pitting in *Ilex aquifolium* and scalariform pitting in *Vitis vinifera*. The average diameter of alternate intervessel pits varied from 2.1 μm in *Betula ermanii* to 7.6 in *Populus fremontii*. Scalariform pits in *Vitis vinifera* were similar in size to the vessel diameter, with average values of 53.6. There was no structural relation between the size and arrangement of the intervessel pits and their pit membrane structure.

Pit membrane porosity—In TEM micrographs, there were no obvious channels spanning pit membranes, although in species with very thin membranes it was difficult to determine if pores were present because of the low electron density of material in the membranes. Images obtained using SEM, however, varied greatly in the apparent porosity of pit membranes. Intact pit membranes of *Laurus nobilis* (Fig. 1A), *Acacia pataczekii*, *Citrus reticulata*, *Olea europaea*, and *Quercus robur* (Fig. 1B) had no visible pores. For *Fraxinus americana* and *Arbutus uva-ursii*, the majority of membranes had no resolvable pores, but pores in a few membranes were up to 30 and 70 nm in diameter, respectively. In several species, pores were of intermediate appearance, with a maximum pore diameter between 50 and 100 nm visible in many, but not all pit membranes, e.g., *Sophora japonica* (Fig. 1C) and *Acer negundo* (Fig. 1D). *Acer pseudoplatanus*, *Adenocarpus decorticans*, *Aesculus hippocastanum*, *Betula pendula*, *Cordia macrostachya*, *Corylus avellana*, *Populus fremontii* (Fig. 1E), *Salix alba* (Fig. 1F), and *Ulmus procera* had membranes with a fragile appearance, numerous pores, and a max pore size between 166 nm and 234 nm.

Pores observed in SEM samples need to be interpreted carefully. In general, porous pit membranes appeared to be more easily damaged or ruptured than nonporous pit membranes, resulting in artificially large pores. There was a propensity for one or more layers of the pit membrane to be removed, leaving the remaining pit membrane appearing more porous than an intact membrane. This preparation artifact was evident in samples where pit membranes of two distinct appearances were observed in close proximity (Fig. 2A, B), and by images of individual pit membranes with one or more layers of the pit membrane removed from one part of the pit membrane, illustrating more porous layers underneath (Fig. 2C). This effect was produced by the splitting of samples in which the secondary and primary walls fracture unevenly between two adjacent bordered pits. Removal of part of the pit membrane layers could

TABLE 2. List of quantitative pit characteristics. Samples are from current and last year's growth ring in 2–4 yr-old branches. Horizontal pit diameter (D_p) and the diameter of the largest pore in pit membranes (D_{max}) were measured from SEM micrographs ($N \geq 40$ pits per species). D_{max} data could not be obtained for species in which pores were not resolvable under SEM. Pit membrane thickness (T_m) and total intervessel cell wall thickness (T_w) were measured from TEM micrographs ($N \geq 25$ pits per species). Air-seeding threshold (P_a) and estimated pit membrane pore diameter (D_e) for seven species perfused with a 10 mM KCl solution ($N = 4$–9); air-seeding values for *Fraxinus americana* and *Sophora japonica* are from Choat et al. (2004). Values are means ± SD.

Species	D_p (μm)	T_m (nm)	T_w (nm)	P_a (MPa)	D_{max} (nm)	D_e (nm)
Acacia pataczekii	5.28 ± 0.69	1183 ± 442	8018 ± 2620	2.8 ± 0.56		106 ± 21
Acer negundo	4.8 ± 0.40	179 ± 59	2598 ± 629	2.12 ± 0.61	80	148 ± 52
Acer pseudoplatanus	6.10 ± 0.53	176 ± 45	3054 ± 682		189	
Adenocarpus decorticans	5.57 ± 0.92	227 ± 49	2548 ± 526			
Aesculus hippocastanum	6.13 ± 0.63	93 ± 20	3067 ± 378	1.62 ± 0.36	179	186 ± 37
Ailanthus altissima	5.76 ± 0.5	629 ± 150	4778 ± 1327			
Arbutus uva-ursii	4.45 ± 0.49	690 ± 207	2643 ± 1004			
Betula ermanii	2.14 ± 0.29	85 ± 23	2786 ± 478		78	
Betula nigra	2.4 ± 0.30	108 ± 27	2585 ± 653		100	
Betula pendula	2.8 ± 0.33	131 ± 31	2623 ± 461	0.95 ± 0.42	234	340 ± 152
Citrus reticulata	3.17 ± 0.35	480 ± 179	6204 ± 1027			
Cordia macrostachia	4.1 ± 2.85	280 ± 61	4993 ± 1364			
Corylus avellana	5.25 ± 1.19	142 ± 29	2293 ± 520		190	
Fraxinus americana	3.8 ± 0.60	205 ± 45	4324 ± 1102	1.93 ± 0.10	43	152 ± 8
Ilex aquifolium	7.65 ± 4.40	212 ± 65	2522 ± 417		124	
Laurus nobilis	5.5 ± 1.30	577 ± 98	6360 ± 1470	2.8 ± 0.86		113 ± 40
Olea europaea	2.5 ± 0.26	669 ± 130	6316 ± 1136			
Paulownia tomentosa	6.37 ± 0.84	303 ± 55	3294 ± 500			
Populus fremontii	7.6 ± 0.50	100 ± 24	2356 ± 465	1.42 ± 0.72	195	254 ± 141
Quercus robur	5.886 ± 0.75	278 ± 87	2503 ± 562			
Salix alba	6.5 ± 0.40	70 ± 15	2243 ± 278	1.45 ± 0.21	186	203 ± 29
Sambucus nigra	6.511 ± 0.98	117 ± 29	2590 ± 558		112	
Sophora japonica	5.2 ± 1.60	251 ± 58	3552 ± 1232	2.62 ± 0.18	63.3	114 ± 8
Ulmus americana	7.5 ± 0.40	131 ± 64	2946 ± 665		59.91	
Ulmus procera	6.927 ± 0.48	113 ± 22	3669 ± 725		225.2	
Vitis vinifera	53.6 ± 15	185 ± 69	4890 ± 1510		39.33	

be recognized by carefully observing the secondary wall layers surrounding the pit border. Moreover, various layers of the pit membrane could sometimes be identified by a difference in the orientation of the microfibrils (Fig. 2C). Pores were also found more frequently near areas where the pit membrane is ruptured and in pit apertures where the pit border provides little mechanical support. In various species, especially those with a relatively thin pit membrane, it was noticed that part of the pit membrane was aspirated to the pit border.

When all layers of the outer secondary cell wall remained intact, pit membranes of species with thicker membranes appeared as a dense meshwork of microfibrils with no visible pores (Fig. 1A, 1B). However, in some species with relatively thin pit membranes (i.e., <200 nm thickness), large pores were visible through the inner pit aperture of the vessel wall (Fig. 2D). The pit membrane area near the edge of the pit border, which corresponds to the pit membrane annulus, was usually nonporous and distinctly granular in *Acer negundo* (Fig. 1D) and *Betula nigra* (Fig. 1B).

Pit membrane thickness—The thickness of pit membranes varied by more than 25-fold difference in magnitude among the study species, with pit membranes of *Acacia pataczekii* having a mean (±SD) thickness of 1183 (±442) nm, while pit membranes of *S. alba* had an average thickness of 70 (±15) nm. Very thin pit membranes with an average thickness up to 100 nm also occurred in *Aesculus hippocastanum*, *Betula ermanii* (Fig. 3C), and *Populus fremontii* (Fig. 3D). The pit aperture outline could frequently be seen through the thin pit membrane when viewed under SEM (Fig. 1E, 1F). The majority of the species studied had an average thickness between 100 nm and 300 nm. An average thickness above 500 nm was recorded in *Acacia pataczekii*, *Ailanthus altissima*, *Arbutus uva-ursii* (Fig. 3A), *Citrus reticulata* (Fig. 3E), *Laurus nobilis* (Fig. 3B), and *Olea europaea*. Thinner pit membranes (e.g., *Aesculus hippocastanum*, *Salix alba*, *Populus fremontii*) were often almost transparent under TEM, indicating less densely packed material than in pit membranes with higher electron density (e.g., *Laurus nobilis*, *Citrus reticulata*, and *Fraxinus americana*; Fig. 3B, 3E, 3F), or differences in the chemical nature of pit membranes.

Species with membranes that appeared porous using SEM (including *Aesculus hippocastanum*, *Betula ermanii*, *B. nigra*, *B. pendula*, *Corylus avellana*, *Populus fremontii*, *Salix alba*, *Ulmus americana*, and *U. procera*) were relatively thin under TEM, with a pit membrane thickness of less than 150 nm. The average thickness of membranes was significantly related to the average pore diameter ($r^2 = 0.69$, $P < 0.0001$) and to the maximum pore size ($r^2 = 0.70$, $P = 0.002$; Fig. 4A) as observed with SEM. The pit membrane diameter was not significantly related to either thickness ($r^2 = 0.01$, $P = 0.49$) or maximum pore diameter ($r^2 = 0.004$, $P = 0.25$). The torus-margo pit membranes of *Ulmus procera*, which were found in latewood vessels and tracheids, were not measured.

Very thick intervessel cell walls were recorded for *Acacia pataczekii* (8.0 μm ± 2.6), *C. reticulata* (6.4 μm ± 1.0), and *Olea europaea* (6.3 μm ± 1.1). Other species had a mean intervessel cell wall thickness between 2.2 μm (± 0.2) in *Salix alba*, and 4.9 μm (±1.4) in *Cordia macrostachya*. The total intervessel wall thickness between two neighboring vessels was significantly correlated with the average pit membranes thickness ($r^2 = 0.60$, $P < 0.0001$, Fig. 4B). Similar correlations were found for the maximum values of both features. *Arbutus uva-ursii* (Fig. 3A)

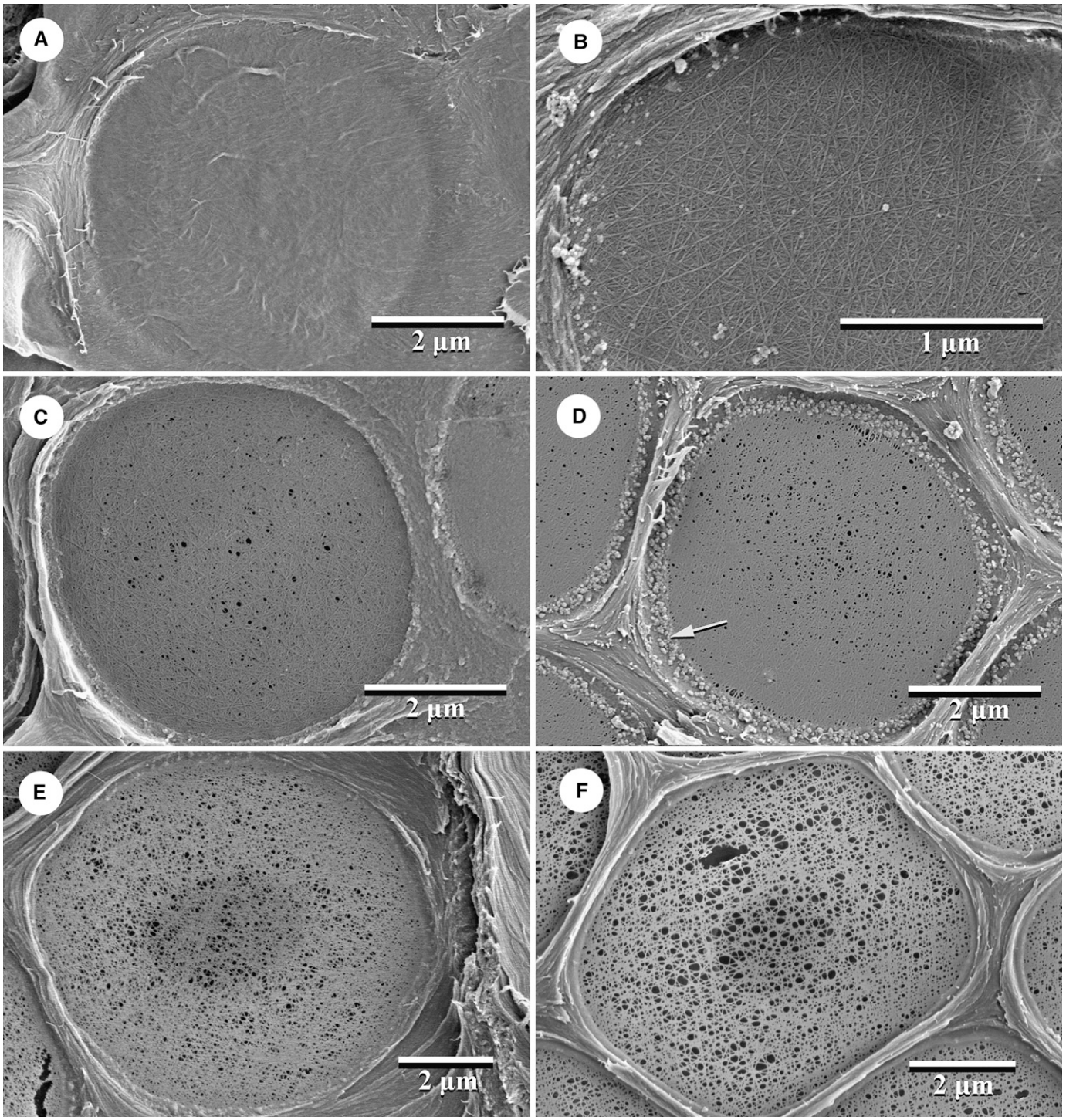

Fig. 1. SEM images of intact intervessel pit membranes in hardwood species showing microfibril orientation and various degrees of porosity. (A) *Laurus nobilis*, nonporous pit membrane. (B) *Quercus robur*, detail of a pit membrane with a random orientation of microfibrils and no visible pores. (C) *Sophora japonica*, pit membrane with pores 25–100 nm in diameter. (D) *Acer negundo*, pit membrane with pores 50–100 nm in diameter and a granular annulus (arrow). (E) *Populus fremontii*, pit membrane with fragile appearance and numerous resolvable pores. The outline of the pit aperture can be seen as a dark, central area of the pit membrane and is a result of the thin, fragile nature of the pit membrane and not an artifact due to beam interaction. (F) *Salix alba*, very porous pit membrane with pores up to 200 nm in diameter. Outline of pit aperture visible as in (E).

appeared to be unusual in having thick pit membranes (on average 690 nm ± 207) and relatively thin intervessel walls (on average 2.64 µm ± 1). In half of the species studied, the middle lamella and primary cell wall were visible in the vessel cell wall as a slightly electron-dense layer (Fig. 3A, 3C, 3E, 3F). For most species, the thickness of this layer was larger than the

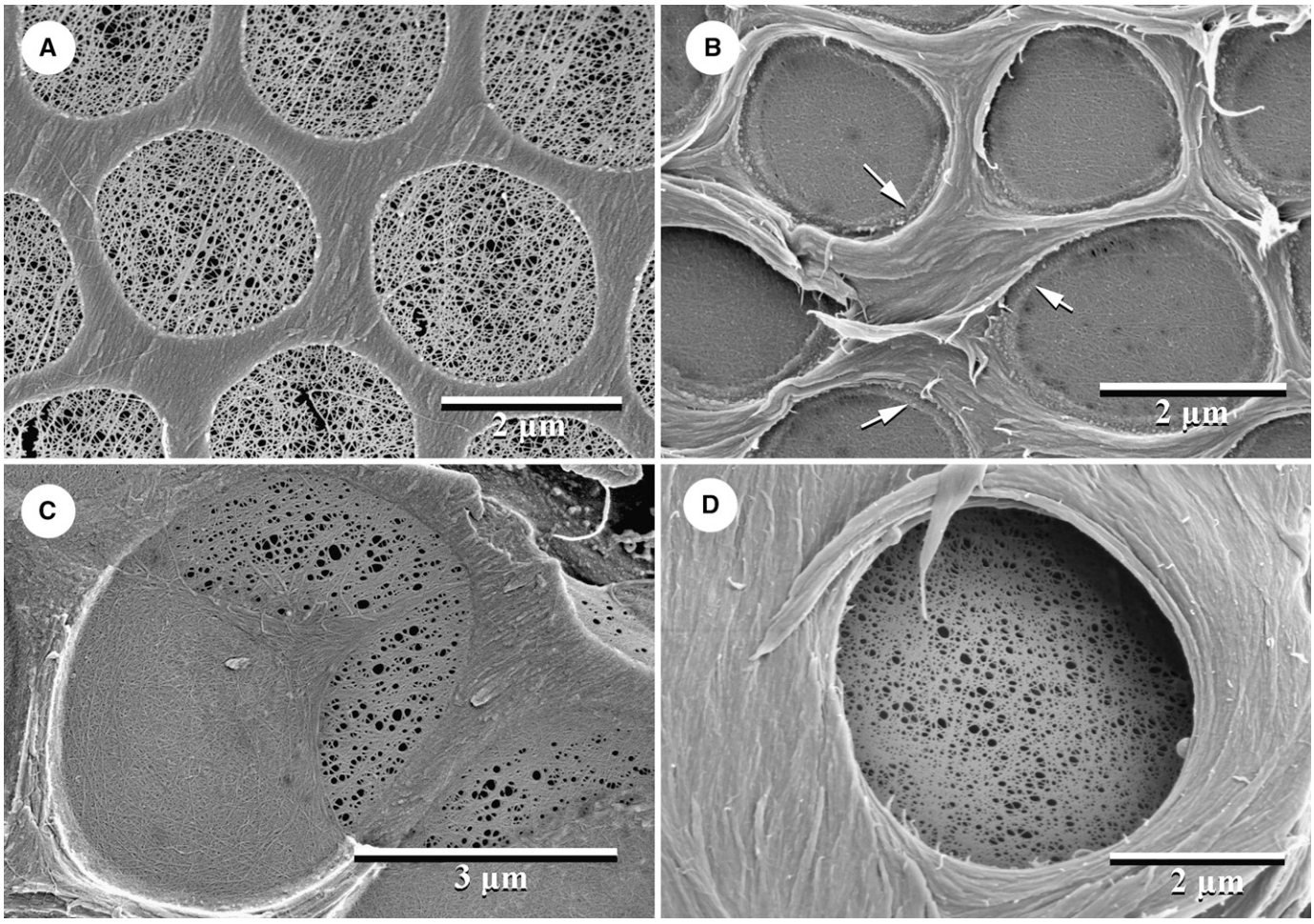

Fig. 2. SEM images of intervessel pits showing varying degrees of porosity. (A) *Betula nigra*, thin, porous pit membrane layers after partial removal of the pit membrane and secondary cell wall. (B) *Betula nigra*, alternate pitting with intact pit membranes, annulus (arrows) visible near the pit border. (C) *Sophora japonica*, layers partially stripped from part of the membrane reveal a more porous structure with different microfibril orientation than intact areas with random microfibril arrangement. (D) *Salix alba*, pores visible in intact pit membrane viewed through the inner pit aperture.

average pit membrane thickness. The thickness of the primary cell wall and middle lamella was related to the pit membrane thickness ($r^2 = 0.66$, $P = 0.01$, Fig. 4C) and was related to the total intervessel wall thickness ($r^2 = 0.41$, $P < 0.001$).

Microfibrils—The outermost cellulose microfibrils in pit membranes were oriented randomly (Fig. 1B), and layers underneath usually had a more parallel arrangement (Fig. 2A, 2C). The microfibrils were frequently incrusted by amorphous material. Sometimes microfibrils seemed to extend from its pit membrane layer into its surrounding vessel wall. These microfibrils may have detached from the pit membrane and deposited on the secondary vessel wall during sample preparation. The mean microfibril thickness for all species studied based on SEM was on average 20.17 nm (±4.32). In samples of *Citrus reticulata* and *Laurus nobilis*, the microfibrils were not well defined, probably because of incrustations on the pit membrane. Electron-dense dots were consistently observed in TEM sections of transparent pit membranes of *Acer pseudoplatanus, Adenocarpus decorticans, Betula ermanii* (Fig. 3C), *B. pendula, Cordia macrostachya, Ilex aquifolium*, and *Sambucus nigra*. Although these dots were similar in size as the microfibrils measured using SEM, significant differences were found for *Aesculus hippocastanum*, *Betula ermanii*, and *Populus fremontii*, suggesting that the electron-dense dots as observed in TEM sections could either be microfibrils or granular inclusions of variable size.

Pit membrane ultrastructure—Intervessel pit membranes were composed of uniformly deposited fibrillar material, frequently with a less electron-dense inner layer than the outer layers of the pit membrane. Pit membranes with a clearly layered composition were found in most but not all intervessel pits of *Fraxinus americana* (Fig. 3F), *Laurus nobilis* (Fig. 3B), *Olea europaea*, *Paulownia tomentosa*, and *Ulmus procera*. All species studied had an annulus near the outer edge of the pit membrane. In general, the annulus was more electron dense, but thinner than the central area of the membrane. While intervessel pit membranes were transparent in most species, most pit membranes in *Laurus nobilis* (Fig. 3B) and *Citrus reticulata* (Fig. 3E) were more electron dense than other parts of the intervessel cell wall.

Air-seeding thresholds—Single vessel air-seeding measurements ranged from 0.9 to 2.8 MPa for nine species examined. There were correlations between air-seeding threshold (P_a) and

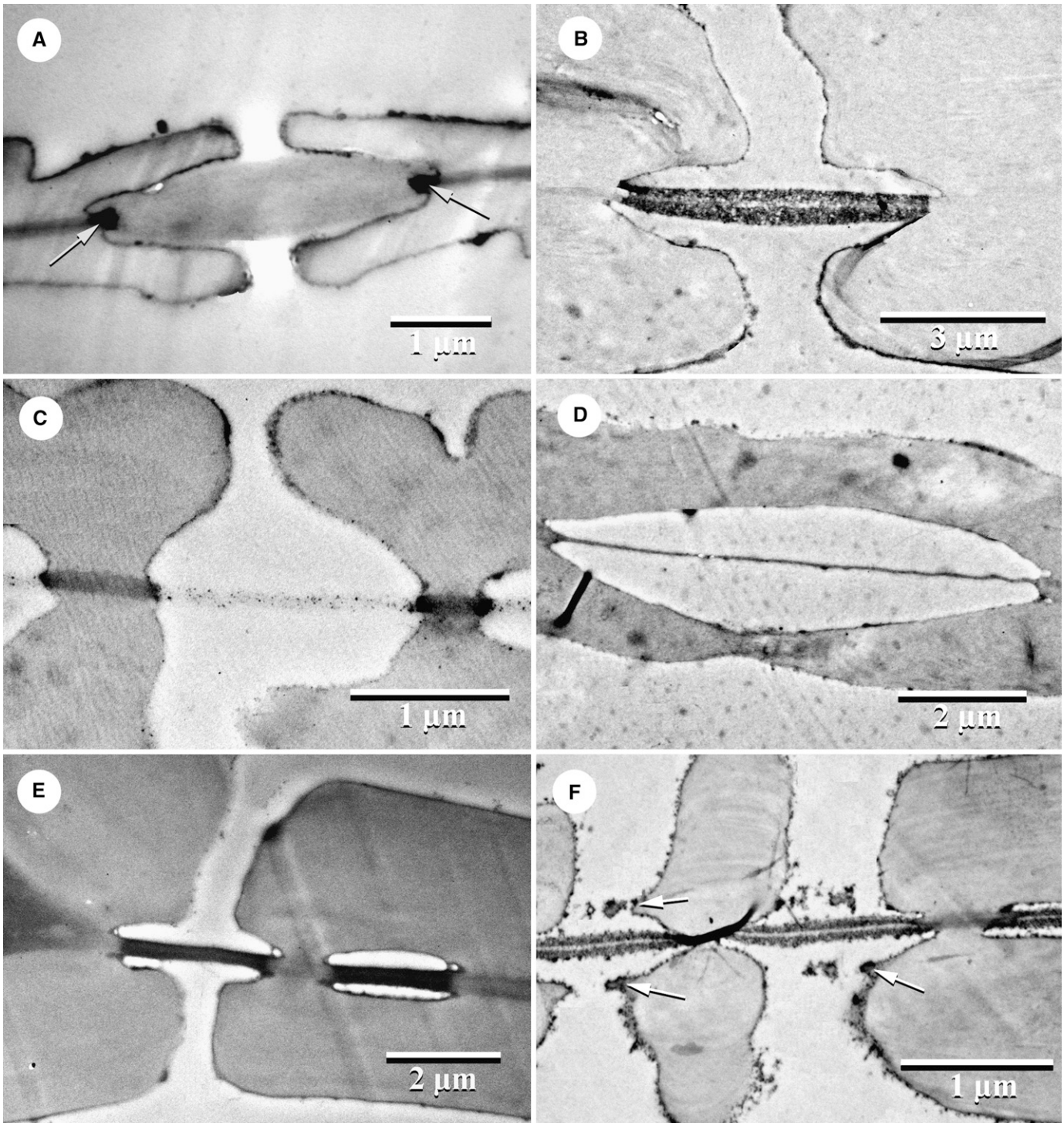

Fig. 3. TEM images of intervessel pit membranes in hardwood species showing structural variation. All images are from transverse, ultrathin (60–90 nm) sections. (A) *Arbutus uva-ursii*, thick pit membrane up to 800 nm, distinct, electron-dense annulus (arrows), and thin (<2 µm) intervessel wall. (B) *Laurus nobilis*, thick pit membrane up to 680 nm with electron-dense material and a slightly more transparent inner layer. (C) *Betula ermanii*, thin (80–90 nm), transparent pit membrane. (D) *Populus fremontii*, thin (<60 nm) pit membrane. The pit apertures are not visible because the pit is not cut in its center. (E) *Citrus reticulata*, thick (up to 320 nm), electron-dense pit membranes and thick intervessel walls. (F) *Fraxinus americana*, pit membranes (ca. 160 nm in thickness) composed of a transparent inner layer and dark outermost layers, weakly developed vestures (arrows) near edge of pit borders.

maximum pore diameter ($r^2 = 0.87$, $P = 0.005$, Fig. 4D), and mean pore diameter ($r^2 = 0.79$, $P = 0.006$, Fig. 4E), and pit membrane thickness ($r^2 = 0.52$, $P = 0.03$). Because air seeding will always occur at the largest pore first, pore diameters calculated from air-seeding values should represent the maximum rather than the average pore diameter. When circular pore

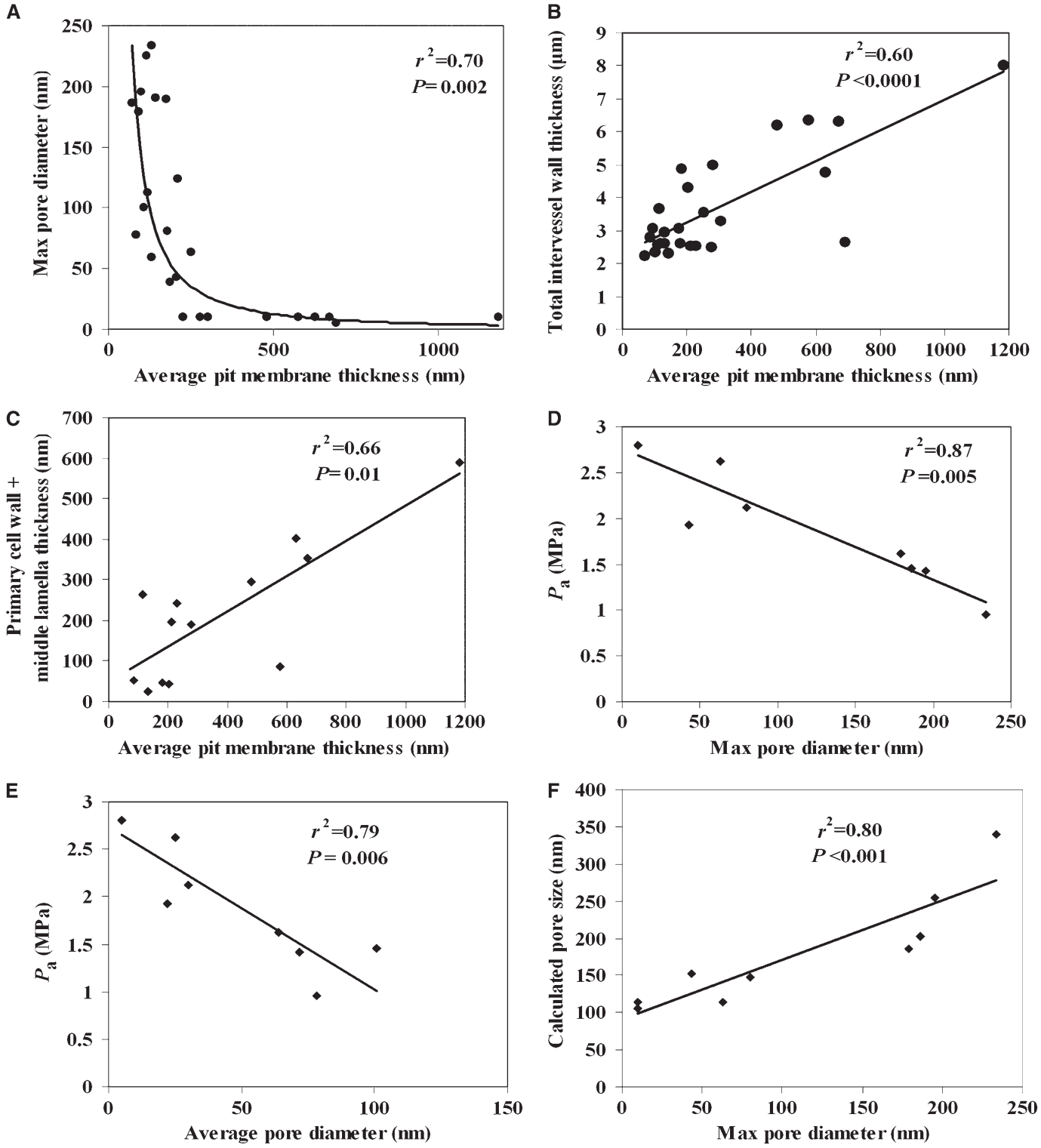

Fig. 4. Relationships between pit membrane characteristics as measured with SEM and TEM and air-seeding thresholds for hardwood species. For species in which pores were not resolvable with SEM, maximum pore diameter was set at 10 nm, and average pore diameter was set at 5 nm. (A) Average pit membrane thickness as measured with TEM ($N \geq 25$ pits per species) vs. maximum pore diameter measured with SEM ($N \geq 40$ pits per species) for 26 hardwood species. (B) Relationship of average pit membrane thickness to total intervessel wall thickness measured with TEM for 26 hardwood species ($N \geq 25$ measurements per species). (C) Relationship of average pit membrane thickness to primary cell wall and middle lamella thickness as measured with TEM ($N \geq 25$ measurements per species) for 13 hardwood species. (D) Relationship between air-seeding threshold (P_a) ($N = 4$–9 per species) and maximum pore diameter measured with SEM for nine hardwood species. (E) Relationship between air-seeding threshold (P_a) ($N = 4$–9 per species) and average pore diameter measured with SEM for nine hardwood species. (F) Relationship between theoretical pore diameter calculated from air-seeding thresholds ($N = 4$–9 per species) and maximum pit membrane porosity measured with SEM ($N \geq 40$ pits per species) for nine hardwood species.

diameters were calculated from P_a, there were significant correlations between calculated diameters and maximum ($r^2 = 0.8$, $P < 0.001$, Fig. 4F) and mean pore diameter ($r^2 = 0.6$, $P < 0.0001$). Calculated pore diameters were always larger than the maximum pore diameters measured from SEM images.

DISCUSSION

There was wide variation in the structure of intervessel pit membranes of the 26 angiosperm species examined, especially with respect to differences in thickness and maximum pore size. This variation is consistent with the finding of Sano (2004, 2005), who observed significant interspecific variation in the pit membrane structure of temperate hardwood species. Here we present the first record of variation in pit membrane structure in hardwood species from a range of provenances including riparian, temperate, and Mediterranean environments. This large variation in pit structure is of potentially great adaptive value given the important role of pit membranes in xylem transport (Zimmermann, 1983; Choat et al., 2008). However, because of the concerns arising from artifacts in pit membrane structure caused by sample preparation for electron microscopy, it is prudent to deal with methodological concerns before further discussing the ecological and physiological implications of our results. In particular, we emphasize the value of complimentary techniques such as SEM, TEM, and air-seeding thresholds in evaluating the fine structure of pit membranes.

Pit membrane structure and methodological concerns—In the current study, pit membranes of many species had visible pores when viewed with SEM. Some images revealed that layers of the pit membrane may be easily removed during preparation, substantially increasing the apparent membrane porosity. Previous studies have shown that there are multiple layers of microfibrils in intervessel pit membranes of hardwood species with various layers often having different orientation of microfibrils (Schmid and Machado, 1968; Sano, 2005). It appears that layers of the primary wall, which make up the pit membrane, may be easily removed when wood sections are split to expose pit fields. From this, it is tempting to conclude that many of the large pores observed with SEM are the result of layers being removed from the membrane. However, there were many instances in which pores could be seen in pit membranes that appeared intact, and in some cases, large pores were visible in pit membranes viewed through the inner aperture of the pit canal of an undamaged secondary wall (Fig. 2D). These observations indicate that pores of large diameter were not always caused by removal of cell wall material.

In comparing the TEM and SEM results of this study, pit membranes that appeared more porous in scanning electron micrographs (*Aesculus hippocastanum*, *Betula ermanii*, *B. nigra*, *B. pendula*, *Corylus avellana*, *Populus fremontii*, *Salix alba*, *Ulmus americana*, and *U. procera*) were also the thinnest membranes when viewed with TEM. Pores spanning the breadth of pit membranes were not discernable with TEM, perhaps because most pit membrane pores are narrower than the TEM sections (60–90 nm) (Schmitz et al., 2007). In pit membranes with a greater mean thickness than 250 nm, pores were generally not resolvable in SEM images (Fig. 4A). It is assumed that the pathway of pores through thicker pit membranes is more complex than those through thin membranes because of the differing orientation of successive layers of microfibrils and that pores of thicker membranes are therefore easily obscured when the membrane is dried. Moreover, the width of the microfibrils as measured using SEM does not seem to be associated with pit membrane thickness, indicating that the pit membrane thickness is mainly determined by the number of microfibril layers.

Air-seeding thresholds should measure the pressure difference at which gas will penetrate pit membranes separating an embolized and functional vessel under natural conditions. The correlation of P_a with maximum pore diameter and mean pit membrane thickness shows that pit membrane characteristics observed with SEM and TEM bear a consistent relationship to the ability of pit membranes to resist air seeding. The relationship between maximum and theoretical pore sizes (Fig. 4F) suggests that SEM observations of porosity bear a consistent relationship with in situ porosity of membranes. However, maximum pore diameters observed with SEM were always 2–4 times smaller than theoretical maximum pore diameters, particularly in species with thicker membranes and no resolvable pores in SEM images. This finding suggests that (1) pores become enlarged by stretching during air seeding due to the pressure difference across the membrane and/or (2) that the large pores responsible for air seeding are rare and not often detected with SEM (Choat et al., 2003, 2004). Therefore, SEM and TEM measurements of membrane structure appear to provide reliable information on the relative ease with which gas can penetrate between vessels, i.e., thinner pit membranes will be more easily damaged or are more likely to have naturally occurring large pores than thick membranes. However, the absolute values for pore diameter derived from SEM should be treated as suspect and complemented with other techniques such as air seeding and particle perfusion experiments (Choat et al., 2005). It would be interesting to know the appearance of the pit membrane after the air-seeding experiments. Previous experiments did not reveal any evidence that pit membranes of *Fraxinus americana* and *Sophora japonica* ruptured when exposed to high pressures (6 MPa), suggesting that at least in these species deflection and stretching of the pit membranes does not result in irreversible changes in pit membrane porosity (Choat et al., 2004).

Physiological and ecological implications of variation in pit structure—The large variation in pit membrane thickness and average pit membrane pore diameter observed in this study is expected to have a significant effect on the area-specific hydraulic resistance of the pit membrane (r_{mem}). Given that pit resistance is estimated to account for half of total xylem resistance, this variation could influence hydraulic efficiency of the xylem significantly. However, recent evidence from physiological studies has suggested that the trade-off between vulnerability to embolism and hydraulic resistance does not take place at the pit level (Wheeler et al., 2005). Across a range of species, there was no correlation between r_{mem} and vulnerability to embolism; species with lower r_{mem}, suggesting higher average porosity, were not necessarily more vulnerable to embolism (Hacke et al., 2006). An explanation for this result is based on the hypothesis that large pit membrane pores responsible for air seeding are rare, i.e., they only occur in one of the many pit membranes that connect two vessels (Choat et al., 2003). In this situation, vulnerability to embolism scales with the total surface area of pit membrane connecting vessels, with the chance of a large pore occurring increasing in a stochastic fashion with increasing surface area. The "pit area" hypothesis is supported by a strong relationship between pit membrane area between vessels and vulnerability to embolism (Wheeler et al., 2005).

In light of new evidence demonstrating large variation in pit membrane structure across species, it seems unlikely that pit structure is playing a negligible role in this trade-off. In species with thinner, more porous membranes, there should be a greater chance of having a large pore for a given area of membrane overlap compared with species that have thicker membranes. Therefore, we would expect significant variation in vulnerability to embolism between species with different membrane thickness and porosity even if overlap area of pit membrane is constant. In support of this, plots of vulnerability to embolism vs. pit overlap area show considerable variation in vulnerability to embolism for a given pit area (Hacke et al., 2006), suggesting that variation in pit structure explains significant differences in vulnerability to embolism within a narrow band of pit area. However, caution must be exercised when using pit anatomical measurements to directly infer physiological function. For instance, previous measurements indicate that *Laurus nobilis* is more vulnerable to embolism than *Acer negundo*, which has thinner and more porous pit membranes (Hacke and Sperry, 2003). It is now apparent that vulnerability to embolism results from the interaction of both tissue level properties (vessel diameter, length, and overlap area) and pit level structure (porosity, thickness, and aperture dimensions). Further work incorporating hydraulic measurements is required to unravel the relative importance of pit level and tissue level structure in the ability of plants to persist in differing environments and to assess the adaptive value of the large variation observed in pit membrane structure in this study.

Differences in thickness are likely to influence the degree to which pit membranes are damaged or altered structurally by mechanical deformation. Deflection and stretching of pit membranes has been shown to result from large pressure differences that develop between embolized and functional xylem vessels (Choat et al., 2004). The thickness of pit membranes is expected to play a significant role in the degree to which pit membranes would be susceptible to rupture or enlargement of existing pores. The relationship between P_a and pit membrane thickness suggests that there is little gain in resistance to air seeding after a certain thickness has been reached; there was no difference in P_a between *Laurus nobilis* and *Acacia patazcekii* despite a twofold difference in thickness. This observation may be because there was a larger area of pit membrane (more pits) between vessels of *Acacia patazcekii* and therefore a greater chance of a large pore being present (see earlier pit area hypothesis). The size of the pit aperture is also likely to be important in determining the likelihood of pit membrane damage due to stretching, because a larger aperture will leave more of the pit membrane unsupported. Thus, species such as *Salix alba* that have thin membranes and wide pit apertures should be more easily damaged than species with thick membranes and small pit apertures such as *Laurus nobilis*.

The correlation between pit membrane thickness and secondary cell wall thickness provides some insights into the structural basis of the strong correlation between vulnerability to cavitation and wood density (Hacke et al., 2001; Cochard et al., 2008). Conduits with thicker secondary walls for a given lumen diameter (thickness to span ratio) are more resistant to implosion resulting from pressure differences that develop between embolized and functional conduits. Hacke et al. (2001) demonstrated that cavitation generally occurs via air seeding before the pressure difference across the pitted wall is great enough to cause implosion. Some structural features must underlie the scaling between air-seeding thresholds and vessel implosion, lowering the risk of permanent damage to xylem conduit. If thinner pit membranes are associated with increased vulnerability to cavitation, a structural link is provided for the correlative relationship between thickness to span ratio and vulnerability to cavitation. Of course, other structural features such as pit overlap area (Wheeler et al., 2005) and fiber wall thickness (Jacobsen et al., 2005; Pratt et al., 2007) must also play a role in what is likely to be a complex relationship between vulnerability to cavitation and wood density.

Vestured pits occur in the three legume species studied (*Acacia patazcekii*, *Adenocarpus decorticans*, and *Sophora japonica*). In addition, sparsely developed vestures occur in *Fraxinus americana* (Fig. 3F), while all other species examined had nonvestured pits (Jansen et al., 2001). No apparent correlation is found between the presence of vestures and structural aspects such as pit membrane thickness. However, there is a significant relationship ($P = 0.0012$) between the air-seeding threshold and the distribution of vestures: air-seeding thresholds in *Acacia patazcekii*, *Sophora japonica*, *Fraxinus americana*, and two additional legume species (*Cladrastis sinensis*, *Robinia pseudoacacia*; S. Jansen, personal observation) have an average air-seeding threshold of 2.39 MPa ± 0.61 ($N = 30$), while the average air-seeding threshold for all nonvestured pit samples tested in this study is 1.71 MPa ± 0.88 ($N = 28$). Interestingly, intervessel pit membranes in *Cladrastis sinensis* and *Robinia pseudoacacia* are relatively thin (on average 119 ± 25 nm and 119 ± 35 nm, respectively; SJ personal observation), indicating that vestures may support the pit membrane and reduce the degree to which the pit membrane can be deflected, which in turn increases the air-seeding value (Zweypfenning, 1978; Jansen et al., 2003, 2004b; Choat et al., 2004). Species without vestured pits, however, seem to require a thick pit membrane to provide a high air-seeding value. Further study on a larger number of species with vestured pits is required to generalize the hydraulic safety that vestured pits may provide.

LITERATURE CITED

BAUCH, J., W. LIESE, AND R. SCHULTZE. 1972. The morphological variability of the bordered pit membranes in gymnosperms. *Wood Science and Technology* 6: 165–184.

CHOAT, B., M. BALL, J. LULY, AND J. HOLTUM. 2003. Pit membrane porosity and water stress-induced cavitation in four co-existing dry rainforest tree species. *Plant Physiology* 131: 41–48.

CHOAT, B., T. W. BRODIE, A. R. COBB, M. A. ZWIENIECKI, AND N. M. HOLBROOK. 2006. Direct measurements of intervessel pit membrane hydraulic resistance in two angiosperm tree species. *American Journal of Botany* 93: 993–1000.

CHOAT, B., A. COBB, AND S. JANSEN. 2008. Structure and function of bordered pits: New discoveries and impacts on whole plant hydraulic function. *New Phytologist* 177: 608–626.

CHOAT, B., S. JANSEN, M. A. ZWIENIECKI, E. SMETS, AND N. M. HOLBROOK. 2004. Changes in pit membrane porosity due to deflection and stretching: the role of vestured pits. *Journal of Experimental Botany* 55: 1569–1575.

CHOAT, B., E. C. LAHR, P. J. MELCHER, M. A. ZWIENIECKI, AND N. M. HOLBROOK. 2005. The spatial pattern of air seeding thresholds in mature sugar maple trees. *Plant, Cell & Environment* 28: 1082–1089.

COCHARD, H., S. T. BARIGAH, M. KLEINHENTZ, AND A. ESHEL. 2008. Is xylem cavitation resistance a relevant criterion for screening drought resistance among *Prunus* species? *Journal of Plant Physiology* 165: 976–982.

DUTE, R., L. HAGLER, AND A. BLACK. 2008. Comparative development of intertracheary pit membranes in *Abies firma* and *Metasequoia glyptostroboides*. *International Association of Wood Anatomists Journal* 29: 277–289.

DUTE, R. R., A. L. MARTIN, AND S. JANSEN. 2004. Intervascular pit membranes with tori in wood of *Planera aquatica* J.F. Gmel. *Journal of the Alabama Academy of Science* 75: 7–21.

DUTE, R. R., AND A. E. RUSHING. 1987. Pit pairs with tori in the wood of *Osmanthus americanus* (Oleaceae). *International Association of Wood Anatomists Bulletin* 8: 237–244.

HACKE, U. G., AND J. S. SPERRY. 2003. Limits to xylem refilling under negative pressure in *Laurus nobilis* and *Acer negundo. Plant, Cell & Environment* 26: 303–311.

HACKE, U. G., J. S. SPERRY, S. D. POCKMAN, AND K. MCCULLOH. 2001. Trends in wood density and structure are linked to prevention of xylem implosion by negative pressure. *Oecologia* 126: 457–461.

HACKE, U. G., J. S. SPERRY, J. K. WHEELER, AND L. CASTRO. 2006. Scaling of angiosperm xylem structure with safety and efficiency. *Tree Physiology* 26: 619–701.

JACOBSEN, A. L., F. W. EWERS, R. B. PRATT, W. A. PADDOCK III, AND S. D. DAVIS. 2005. Do xylem fibers affect vessel cavitation resistance? *Plant Physiology* 139: 546–556.

JANSEN, S., P. BAAS, P. GASSON, F. LENS, AND E. SMETS. 2004b. Variation in xylem structure from tropics to tundra: Evidence from vestured pits. *Proceedings of the National Academy of Sciences, USA* 101: 8833–8837.

JANSEN, S., P. BAAS, P. GASSON, AND E. SMETS. 2003. Vestured pits—Do they promote safer water transport? *International Journal of Plant Sciences* 164: 405–413.

JANSEN, S., P. BAAS, AND E. SMETS. 2001. Vestured pits: Their occurrence and systematic importance in eudicots. *Taxon* 50: 135–167.

JANSEN, S., B. CHOAT, S. VINCKIER, F. LENS, P. SCHOLS, AND E. SMETS. 2004a. Intervascular pit membranes with a torus in the wood of *Ulmus* (Ulmaceae) and related genera. *New Phytologist* 163: 51–59.

JANSEN, S., A. PLETSERS, AND Y. SANO. 2008. The effect of preparation techniques on SEM-imaging of pit membranes. *International Association of Wood Anatomists Journal* 29: 160–178.

JANSEN, S., Y. SANO, B. CHOAT, D. RABAEY, F. LENS, AND R. R. DUTE. 2007. Pit membranes in tracheary elements of Rosaceae and related families: New records of tori and pseuotori. *American Journal of Botany* 94: 503–514.

KARNOVSKY, M. J. 1965. A formaldehyde–glutaraldehyde fixative of high osmolality for use in electron microscopy. *Journal of Cell Biology* 27: 137–138.

LIESE, W., AND M. FAHNENBROCK. 1952. Elektronenmikroscopische Untersuchungen über den Bau der Hoftüpfel. *Holz Roh- Werkstoff* 10: 197–201.

MELCHER, P. J., M. A. ZWIENIECKI, AND N. M. HOLBROOK. 2003. Vulnerability of xylem vessels to cavitation in sugar mapple. Scaling from individual vessels to whole branches. *Plant Physiology* 131: 1775–1780.

O'BRIEN, T. P., N. FEDER, AND M. E. MCCULLY. 1964. Polychromatic staining of plant cell walls by toluidine blue O. *Protoplasma* 59: 368–373.

OHTANI, J., AND S. ISHIDA. 1978. Pit membrane with torus in dicotyledonous woods. *Journal of the Japanese Wood Research Society* 24: 673–675.

PESACRETA, T. C., L. H. GROOM, AND T. G. RIALS. 2005. Atomic force microscopy of the intervessel pit membrane in the stem of *Sapium sebiferum* (Euphorbiaceae). *International Association of Wood Anatomists Journal* 26: 397–426.

PETTY, J. A., AND R. D. PRESTON. 1969. The dimensions and number of pit membranes pores in conifer wood. *Proceedings of the Royal Society, B, Biological Sciences* 172: 137–151.

PRATT, R. B., A. L. JACOBSEN, F. W. EWERS, AND S. D. DAVIS. 2007. Relationships among xylem transport, biomechanics, and storage in stems and roots of nine Rhamnaceae species of the California chaparral. *New Phytologist* 174: 787–798.

ROOD, S. B., S. PATINO, K. COOMBS, AND M. T. TYREE. 2000. Branch sacrifice: Cavitation-associated drought adaptation of riparian cottonwoods. *Trees—Structure and Function* 14: 248–257.

SANO, Y. 2004. Intervascular pitting across the annual ring boundary in *Betula platyphylla* var. *japonica* and *Fraxinus mandshurica* var. *japonica. International Association of Wood Anatomists Journal* 25: 129–140.

SANO, Y. 2005. Inter- and intraspecific structural variations among intervascular pit membranes as revealed by field-emission scanning electron microscopy. *American Journal of Botany* 92: 1077–1084.

SANO, Y., Y. KAWAKAMI, AND J. OHTANI. 1999. Variation in the structure of intertracheary pit membranes in *Abies sachalinensis*, as observed by field-emission scanning electron microscopy. *International Association of Wood Anatomists Journal* 20: 375–388.

SCHMID, R. 1965. The fine structure of pits in hardwoods. *In* W. A. Côté [ed.], Cellular ultrastructure of woody plants, 291–304. Syracuse University Press, Syracuse, New York, USA.

SCHMID, R., AND R. D. MACHADO. 1968. Pit membranes in hardwoods—Fine structure and development. *Protoplasma* 66: 185–204.

SCHMITZ, N., S. JANSEN, A. VERHEYDEN, J. G. KAIRO, H. BEECKMAN, AND N. KOEDAM. 2007. Anatomical and ecological variation in the scaling of intervessel pits in wood of two Kenyan mangrove species. *Annals of Botany* 100: 271–281.

SHANE, M. W., M. E. MCCULLY, AND M. J. CANNY. 2000. Architecture of branch-root junctions in maize: Structure of the connecting xylem and the porosity of pit membranes. *Annals of Botany* 85: 613–624.

SOKAL, R. R., AND F. J. ROHLF. 1995. Biometry: The principles and practice of statistics in biological research, 3rd ed. W. H. Freeman, New York, New York, USA.

THOMAS, R. J. 1969. The ultrastructure of southern pine bordered pit membranes as revealed by specialized drying techniques. *Wood and Fiber* 1: 110–123.

THORSCH, J. A. 2000. Vessels in Zingiberaceae: A light, scanning, and transmission microscope study. *International Association of Wood Anatomists Journal* 21: 61–76.

TYREE, M. T., AND J. S. SPERRY. 1989. Vulnerability of xylem to cavitation and embolism. *Annual Review of Plant Physiology and Plant Molecular Biology* 40: 19–38.

WHEELER, E. A. 1981. Intervascular pitting in *Fraxinus americana* L. *International Association of Wood Anatomists Bulletin* 2: 169–174.

WHEELER, E. A. 1983. Intervascular pit membranes in *Ulmus* and *Celtis* native to the United States. *International Association of Wood Anatomists Bulletin* 4: 79–88.

WHEELER, J. K., J. S. SPERRY, U. G. HACKE, AND N. HOANG. 2005. Intervessel pitting and cavitation in woody Rosaceae and other vesselled plants: A basis for a safety versus efficiency trade-off in xylem transport. *Plant, Cell & Environment* 28: 800–812.

YANG, K.-C. 1978. The fine structure of pits in yellow birch (*Betula alleghaniensis* Britton). *International Association of Wood Anatomists Bulletin* 4: 71–77.

YANG, K.-C. 1986. The ultrastructure of pits in *Paulownia tomentosa. Wood and Fiber Science* 18: 118–126.

ZIMMERMANN, M. H. 1983. Xylem structure and the ascent of sap. Springer-Verlag, Berlin, Germany.

ZIMMERMANN, M. H., AND C. L. BROWN. 1971. Trees: Structure and function. Springer-Verlag, New York, New York, USA.

ZWEYPFENNING, R. C. V. J. 1978. A hypothesis on the function of vestured pits. *International Association of Wood Anatomists Bulletin* 1: 13–15.